Climatic Change
DOI 10.1007/s10584-013-0833-1

Understanding variations and seasonal characteristics of net primary production under two types of climate change scenarios in China using the LPJ model

Guodong Sun · Mu Mu

Received: 3 May 2012 / Accepted: 28 June 2013

Abstract The approach of conditional nonlinear optimal perturbation related to parameter (CNOP-P) is employed to provide a possible climate scenario and to study the impact of climate change on the simulated net primary production (NPP) in China within a state-of-the-art Lund-Potsdam-Jena dynamic global vegetation model (LPJ DGVM). The CNOP-P, as a type of climate perturbation to bring variation in climatology and climate variability of the reference climate condition, causes the maximal impact on the simulated NPP in China. A linear climate perturbation that induces variation in climatology, as another possible climate scenario, is also applied to explore the role of variation in climate variability in the simulated NPP. It is shown that NPP decreases in northern China and increases in northeastern and southern China when the temperature changes as a result of a CNOP-P-type temperature change scenario. A similar magnitude of change in the spatial pattern variations of NPP is caused by the CNOP-P-type and the linear temperature change scenarios in northern and northeastern China, but not in southern China. The impact of the CNOP-P-type temperature change scenario on magnitude of change of NPP is more intense than that of the linear temperature change scenario. The numerical results also show that in southern China, the change in NPP caused by the CNOP-P-type temperature change scenario compared with the reference simulated NPP is sensitive. However, this sensitivity is not observed under the linear temperature change scenario. The seasonal simulations indicate that the differences between the variations in NPP due to the two types of temperature change scenarios principally stem from the variations in summer and autumn in southern China under the LPJ model. These numerical results imply that NPP is sensitive to the variation in temperature variability. The results influenced by the CNOP-P-type precipitation change scenario are similar to those under the linear precipitation change scenario, which cause

Electronic supplementary material The online version of this article (doi:10.1007/s10584-013-0833-1) contains supplementary material, which is available to authorized users.

G. Sun (✉) · M. Mu
State Key Laboratory of Numerical Modeling for Atmospheric Sciences and Geophysical Fluid Dynamics (LASG), Institute of Atmospheric Physics, Chinese Academy of Sciences, Beijing 100029, China
e-mail: sungd@mail.iap.ac.cn

M. Mu
Key Laboratory of Ocean Circulation and Wave, Institute of Oceanology, Chinese Academy of Sciences, Qingdao 266071, China

Published online: 27 July 2013

the increasing NPP in arid and semi-arid regions of the northern China. The above findings indicate that the CNOP-P approach is a useful tool for exploring the nonlinear response of NPP to climate variability.

1 Introduction

The global climate system will undergo change in the future due to human activities and fossil fuel use (Cao and Woodward 1998; Cramer et al. 2001; Gerber et al. 2004). The Intergovernmental Panel on Climate Change (IPCC) has suggested that the global or regional temperature will increase by 1.4° to 5.8 ° over the twenty-first century (Notaro et al. 2007; IPCC 2007; Wolf et al. 2008; Zeng et al. 2008). The climate system is being induced to change not only in terms of mean climate values, but in climate variability. Observational evidence has shown that there has been be clear variations in climate variability in the past. The IPCC report noted that it was very likely that hot temperature extremes, heat waves and heavy precipitation events would become more frequent in the future. Thus, climate variability (Zwiers and Kharin 1998; Kharin and Zwiers 2000) will also experience variation due to extreme events.

Climate change is a key factor influencing the structure of the terrestrial ecosystem and its carbon cycle. Observational evidence has shown that the terrestrial ecosystem is intensely sensitive to perturbations in temperature and precipitation (Braswell et al. 1997; Lotsch et al. 2003). Simulation results have revealed the response of the terrestrial ecosystem to changes in climatology (Gao et al. 2000). Recently, many studies have found that climate variability plays a key role in the variation observed in terrestrial ecosystems (Cao et al. 2002; Fay et al. 2008). For example, Botta and Foley (2002) demonstrated that climate variability results in the changes in ecosystem structure, soil carbon and vegetation carbon. Mitchell and Csillag (2001) also emphasized that climate variability can influence the stability of the grasslands, and result in high uncertainty in estimating the net primary production (NPP) of grasslands.

China is situated in the Asian Monsoon region, and the climate conditions in China have changed due to human activities and fossil fuel use (IPCC 2007; Wu et al. 2010). It is important to explore the impacts of climate change on terrestrial ecosystems. There are many investigations addressing these impacts using climate data simulated by general circulation models (GCMs, Ni et al. 2000; Wu et al. 2010) or sensitivity experiments. However, some studies have indicated that the climate data simulated by GCMs are uncertain (Hu et al. 2003; Collins et al. 2006; Kharin et al. 2007). There are many reports that discuss the estimations arising from the simulation of terrestrial ecosystems using these future climate data, which have indicated that these estimations are uncertain (Berthelot et al. 2005; Wu et al. 2007; Ji et al. 2008). Although GCMs produce multiple climate scenarios, the maximal extent of uncertainty in the simulated terrestrial ecosystem caused by these outputs cannot be measured. Furthermore, discussions regarding the maximal variations in the terrestrial ecosystem that will be caused by the climate change, including those related to climatology and climate variability, are scarce in China.

The approach of conditional nonlinear optimal perturbation (CNOP, Mu et al. 2003) is a nonlinear optimization method. This approach is employed to find the optimal initial perturbation under a given constraint and has been applied to investigate the dynamics of ENSO predictability (Mu et al. 2007a), adaptive observation (Mu et al. 2007b) and grassland ecosystems (Mu and Wang 2007; Sun and Mu 2009). Mu et al. (2010) extended the approach to search for the optimal integrated mode of initial perturbations using model parameter perturbations according to the types of predictability. The CNOP approach related to initial perturbations is referred to as the CNOP-I approach, while that related to model parameter perturbations is designated as CNOP-P approach. The CNOP-P approach has

been applied to discuss ENSO predictability (Mu et al. 2010) and grassland ecosystem stability (Sun and Mu 2011). All of these applications illustrate that the CNOP approach is a useful tool for studying nonlinear systems and indicate that it may be similarly effective for exploring the response of the terrestrial ecosystem to climate change. The CNOP approach has previously been applied to discuss the impact of climate change on soil carbon in China (Sun and Mu 2012).

In this study, our aims were to supply a possible climate scenario; to explore the maximal response of NPP in China to climate change, including climatology and climate variability; and to assess differences between the responses of NPP to two possible climate scenarios using the CNOP-P approach within the state-of-the-art Lund-Potsdam-Jena dynamic global vegetation model (LPJ DGVM, Sitch et al. 2003).

2 The model and methods

2.1 The LPJ model

The DGVM is an effective way to discuss the impact of climate change on terrestrial ecosystems (Cramer et al. 2001; Bonan et al. 2002). The LPJ DGVM is employed in this study due to its broad applicability regarding terrestrial carbon cycles and hydrological cycles (Beer et al. 2007). This model, which originates from the biome model family (Prentice et al. 1992), can simulate the distribution of plant functional types and combine process-based representations of terrestrial vegetation dynamics and land atmosphere carbon and water exchanges. The LPJ DGVM explicitly considers processes, such as photosynthesis, mortality, fire disturbances and soil heterotrophic respiration (Sitch et al. 2003). NPP is the difference between photosynthesis, or gross primary production productivity (GPP) computed based on a coupled photosynthesis–water balance scheme, and autotrophic respiration (Ra). The NPP embodies the production ability of plants under climatic conditions and plays a key role in the terrestrial carbon cycle (Field et al. 1998). The main factors controlling NPP are temperature and precipitation. The remaining carbon is allocated to three pools to produce new tissue. Carbon from dead leaves and roots enters litter; decomposition of litter and soil organic matter is driven by soil temperature and water content. Above-ground litter decomposition depends on air temperature whereas below-ground litter and soil organic matter decomposition are calculated using soil temperature and a modified Arrhenius formulation which implies a realistic decline in apparent Q10 values with temperature, and soil water (Schaphoff et al. 2006).

The input data are information on the monthly precipitation, temperature, wet frequency and cloud cover from the Climatic Research Unit (CRU) from 1901 to 1998 (Mitchell and Jones 2005). The data were generated based on climate data and are fairly credible, especially for some regions where there is a lack of observational data. A dataset of global atmospheric CO_2 concentrations was obtained from a carbon cycle model, also including icecore measurements and atmospheric observations (Kicklighter et al. 1999). The applied soil texture data were based on the Food and Agriculture Organization (FAO) soil data dataset (Zobler 1986).

2.2 Conditional nonlinear optimal perturbation related to parameter (CNOP-P)

In a report by Mu et al. (2010), the CNOP-P approach was proposed according to types of predictability and was applied to study ENSO predictability. The CNOP-P is the parameter perturbation with which the cost function attains its maximal value at the final time. Here,

we will review the derivation of this approach for readers' convenience. Let the nonlinear differential equations be as follows:

$$\begin{cases} \dfrac{\partial U}{\partial t} = F(U,P) \quad U \in R^n, \quad t \in [0,T] \\ U|_{t=0} = U_0 \end{cases} \tag{1}$$

where F is a nonlinear continuous operator and means some combination of U and P, P is a parameter vector, including forcing parameters precipitation and temperature, U is the state variable, and U_0 is an initial value of the state variable. Let M_τ be the propagator of the nonlinear differential equations from the initial time 0 to τ. u_τ is a solution of the nonlinear equations at time τ and satisfies $u(\tau) = M_\tau(u_0, p)$.

Let $U(T; U_0, P)$ and $U(T; U_0, P) + u(T; U_0, p)$ be the solutions of the nonlinear differential Eq. (1) for P and $P + p$, respectively, where P and p are parameter vectors. $u(T; U_0, p)$ describes the departure from the reference state $U(T; U_0, P)$ caused by p. The solutions satisfy the following equations:

$$\begin{cases} U(T;U_0,P) = M_T(U_0,P) \\ U(T;U_0,P) + u(T;U_0,p) = M_T(U_0,P+p) \end{cases}.$$

For a proper norm, $\|\|$, a parameter perturbation, p_δ, is called a CNOP-P if and only if

$$J(p_\delta) = \max_{p \in \Omega} J(p), \tag{2}$$

where

$$J(p) = \|M_T(U_0,P+p) - M_T(U_0,P)\| \tag{3}$$

P is a reference state of parameter, and represents the standard value in the model. p is the perturbation of the reference state, and represents the parameter errors. $p \in \Omega$ is a constraint condition. The CNOP-P is the parameter perturbation whose nonlinear evolution attains the maximum value of the cost function, J, at time T.

2.3 Experimental design

The impacts of climate change on terrestrial ecosystems have been discussed in previous works (Gao et al. 2000; Gerber et al. 2004; Matthews et al. 2005). Their experimental designs were as follows:

$$\frac{\sum_{i=1}^{n}\sum_{j=1}^{12}\left(P_{tem,i,j} + \delta_{tem}\right)}{12 \times n} = \frac{\sum_{i=1}^{n}\sum_{j=1}^{12}\left(P_{tem,i,j}\right)}{12 \times n} + \delta_{tem} \tag{4.1}$$

$$\frac{\sum_{i=1}^{n}\sum_{j=1}^{12}\left(P_{pre,i,j} + \frac{\delta_{pre}}{12}\right)}{n} = \frac{\sum_{i=1}^{n}\sum_{j=1}^{12}\left(P_{pre,i,j}\right)}{n} + \delta_{pre} \tag{4.2}$$

where δ_{tem} or δ_{pre} represents the perturbation and the extent of the increase in temperature or precipitation climatology. P_{tem} is the forcing parameters related to the temperature, and P_{pre} is the forcing parameters related to the precipitation. i and j represent year and month, respectively. The approach only considers the variation in mean state of temperature or

precipitation, and did not consider the variation in temperature or precipitation variability denoted by the standard deviation in comparison with the reference temperature or precipitation variability. The above method supplies a possible climate scenario in which the temperature or precipitation series is superimposed on a constant. We refer to it as a linear climate scenario because the precipitation climatology changes, but the precipitation variability is similar to the reference climate condition from 1961–1970. Considering different perturbations of temperature or precipitation series in every year, we designed a new experiment as follows.

The precipitation or temperature, as the forcing input, is time-dependent. In our study, the monthly precipitation or temperature is considered as a parameter. The temperature or precipitation perturbation, $p_{tem,i}$ or $p_{pre,i}$, as a parameter in the input forcing and time dependent, satisfies the following equations:

$$\frac{\sum_{i=1}^{n}\sum_{j=1}^{12}\left(P_{tem,i,j}+p_{tem,i}\right)}{12\times n}=\frac{\sum_{i=1}^{n}\sum_{j=1}^{12}\left(P_{tem,i,j}\right)}{12\times n}+\delta_{tem} \tag{5.1}$$

$$\frac{\sum_{i=1}^{n}\sum_{j=1}^{12}\left(P_{pre,i,j}+\frac{p_{pre,i}}{12}\right)}{n}=\frac{\sum_{i=1}^{n}\sum_{j=1}^{12}\left(P_{pre,i,j}\right)}{n}+\delta_{pre} \tag{5.2}$$

$$0\le p_{tem,i}\le\sigma_{tem} \tag{6.1}$$

$$0\le p_{pre,i}\le\sigma_{pre} \tag{6.2}$$

The Eqs (5.1) and (5.2) cause variation not only in the temperature or precipitation mean state similar to Eqs (4.1) and (4.2), but probably in the temperature or precipitation variability due to the perturbation in every year. The monthly temperature or precipitation perturbation in a year is the same. Moreover, the perturbation in temperature or precipitation is bounded, which is represented by σ_{tem} or σ_{pre} in Eqs (6.1) and (6.2), indicating the maximum increase in the annual temperature and precipitation. Apparently, the above formulae (Eqs. (5.1), (5.2), (6.1) and (6.2)) also supply a possible climate scenario in which the temperature or precipitation series is superimposed on a nonlinear perturbation series, which we could refer to as a nonlinear climate scenario or CNOP-P-type climate scenario. Although the CNOP-P approach is related to the parameters in the model, the method is employed to explore the response of NPP to climate change, including changes in climatology and climate variability for two reasons. First, the input climate conditions could be regarded as the forcing parameters, which are not similar to state variables in the model but are similar to the physical parameters in the model. Second, the CNOP-P-type temperature or precipitation perturbation is added to the reference temperature or precipitation condition. Based on Eqs. (5.1) and (5.2), the CNOP-P-type perturbation might alter not only the climatology, but the climate variability compared with the reference climate condition.

In the present study, NPP is considered as a variable in the cost function, and temperature and precipitation series are considered as parameter vectors. Based on the spatial distribution of NPP in China, the region corresponding to 103°E-120°E, 24°N-45°N and 120°E-135°E, 40°N-54°N is chosen, where the main plant functional types (PFTs) and NPP are dispersed. n is equal to 10, as in 10 years. The study period was from 1961 to 1970, during which the data are

creditable as the reference climate condition. Because of the climate change occurring in China due to increasing CO_2 concentrations and the findings of other studies, we choose (1) an increase in the mean temperature state of 2° ($\delta_{tem} = 2$) over 10 years, with its perturbation in each year not exceeding 3° ($\sigma_{tem} = 3$); and (2) an increase in the precipitation mean state of 20 % ($\delta_{pre} = \frac{\sum_{i=1}^{n}\sum_{j=1}^{12} P_{pre,i,j}}{n} \times 20\%$) over 10 years, with its perturbation in each year not exceeding 20 % ($\sigma_{pre} = \max_{i=1,n}\{\sum_{j=1}^{12} P_{pre,i,j}\} \times 20\%$) of the maximum precipitation.

Similar to other studies, the LPJ model was run using the CRU data from 1901 to 1930 repeatedly for 1000 model years to achieve an approximate equilibrium in terms of carbon pools and vegetation cover as the initial condition.

Because the cost function may be non-differentiable, some evolutionary algorithms may serve a powerful tool for obtaining the optimal value of the cost function. The evolutionary algorithms were applied to investigate the parameter estimates and the uncertainty of the land surface scheme and extreme events with the MM5 model, or data assimilation (Duan et al. 1992; Kruger 1993; Zhang et al. 2000). In our analyses, the gradients of the cost function about the variables do not exist. Therefore, to obtain the maximum value of cost function, an evolutionary algorithm (differential evolution, DE, Storn and Price 1997) is employed. The advantage of DE lies in obtaining the optimal value of (2) without a gradient. This algorithm has been applied to tune hydrographic model parameters (Chakraborty 2008; Zhang et al. 2009). To effectively obtain the CNOP-P, 200 random initial guess values were chosen. The final optimization was also checked using the DE algorithm again.

3 Numerical results

3.1 Response of NPP to the CNOP-P-type temperature change scenario

3.1.1 Impacts of the temperature change scenario on NPP

To investigate the impact of the temperature change scenario on NPP in China, the LPJ model was driven by the temperature series superimposed with the CNOP-P (Fig. 1a). Compared with the reference state simulated by the LPJ model from 1961 to 1970, NPP is reduced in northern China, while it is increased in northeastern and southern China (Fig. 2a). The numerical results suggest that the greater sensitivity of NPP to the CNOP-P-type temperature change scenario occurs not only in northern China, but in southern China.

3.1.2 Comparison of the impacts of the nonlinear and linear temperature change scenarios on NPP

To analyze the different responses of NPP in China to different types of temperature change scenarios, we compared the NPP influenced by increasing by a 2° increase in temperature in every year from 1961 to 1970, as a linear temperature change scenario, with the NPP affected by the CNOP-P-type temperature change scenario. NPP decreases in northern China, and increases in northeastern China due to the linear temperature change scenario. Though the spatial variation in the two regions is similar for the two types of temperature change scenarios, the extent of variation under the linear temperature change scenario is clearly lower than that under the CNOP-P-type temperature change scenario. The highest diversity occurs in southern China for both types of temperature change scenarios. NPP responds weakly to the linear

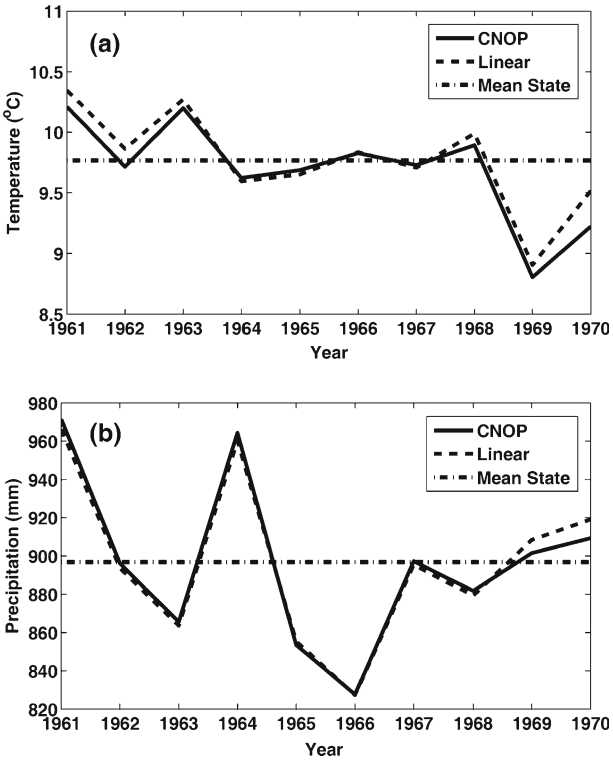

Fig. 1 The temporal variations of the regional averages due to the CNOP-P-type and linear type perturbations for (**a**): temperature; and (**b**): precipitation

temperature change scenario, while it is sensitive to the CNOP-P-type temperature change scenario (Fig. 2 a1 and b1). Regarding the relative change in NPP, the effects are analogous to the two types of temperature change scenarios in northern China. The result is similar to that reported by Gao et al. (2000). The numerical results indicate that the southern China may be a region that is sensitive to nonlinear climate change. However, the character is obscured in southern China to the linear climate change.

To interpret the reasons underlying the variations in NPP in light of the different types of temperature change scenarios, we provide the gross primary productivity (GPP) and the autotrophic respiration (Ra). In the LPJ model, the NPP satisfies the following relationship:

$$\mathrm{NPP} = \mathrm{GPP} - \mathrm{Ra}.$$

Figure 2c1 and d1 show that the spatial changes in GPP due to the different types of temperature change scenarios are similar. In northern China, in which includes arid and semi-arid regions, GPP decreases. The increase of temperature induces increasing evapotranspiration, and the water content decreases in the soil. The above effects and the shortage of rainfall inhibit photosynthesis, so GPP decreases. In northeastern and southern China, despite the temperature increases, the rainfall is sufficient to lead to an enhancement of photosynthesis. In both regions, GPP increases (Fig. 2c1 and d1).

The responses of Ra to the different types of temperature change scenarios are different in southern China. The CNOP-P-type temperature change scenario results in a reduction of Ra,

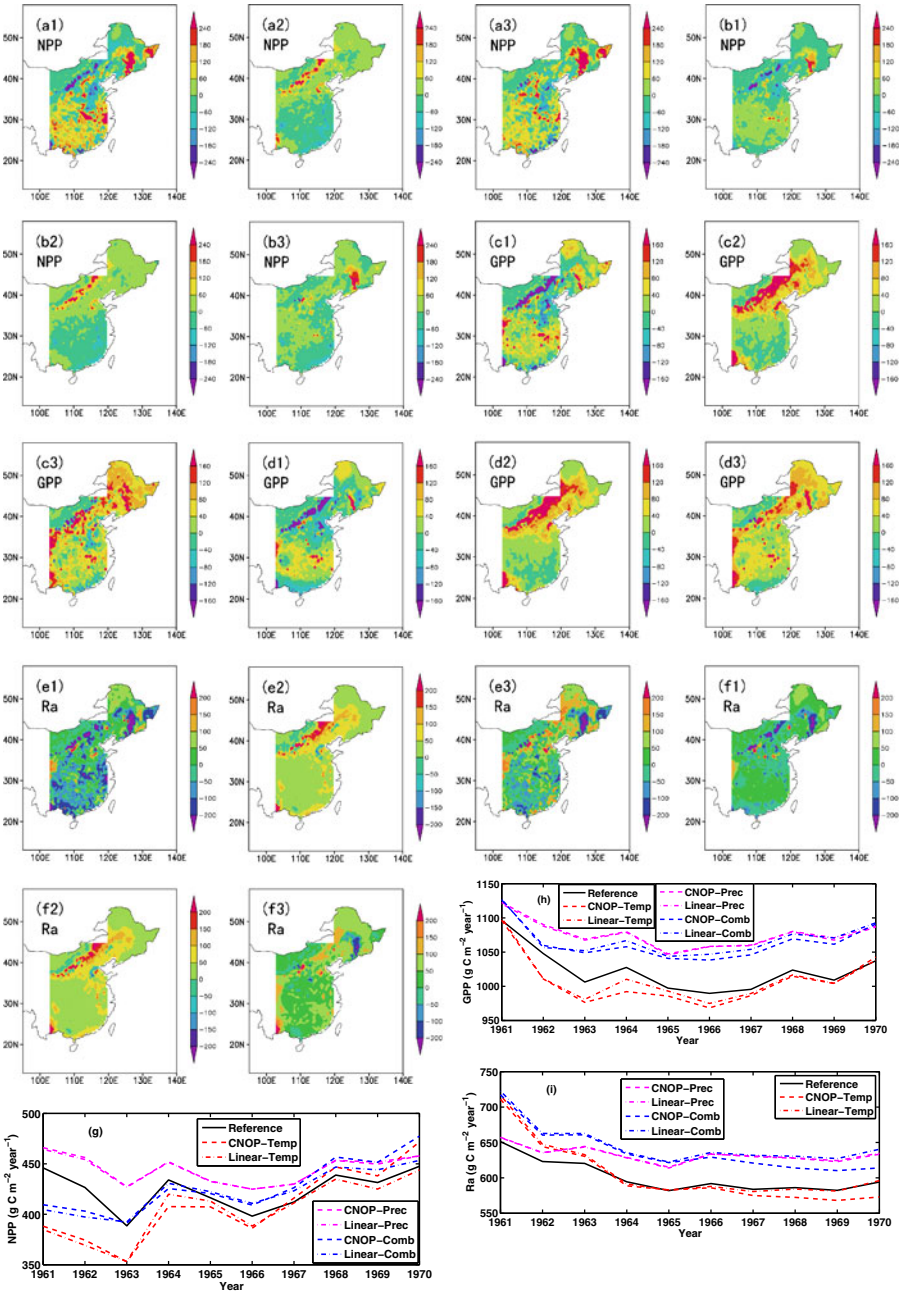

Fig. 2 (a1-b1): The spatial and temporal variations in the net primary production (NPP); (c1-d1): gross primary production (GPP); and (e1-f1): autotrophic respiration (Ra) in comparison with the reference state (unit: g C m^{-2} year^{-1}) for the temperature case. (a1, c1, e1): The CNOP-P-type temperature changes; (b1, d1, f1): the linear type temperature changes. (a2–f2): same as in (a1–f1), but for precipitation case. (a3–f3): same as in (a1–f1), but for the combined temperature and precipitation scenario. "Reference" means the reference state; "CNOP-Temp" means for temperature case using the CNOP approach; "CNOP-Prec" means for precipitation case using the CNOP approach; "CNOP-Comb" means for the combined temperature and precipitation scenario using the CNOP approach. "Linear" means for linear case

while the linear temperature change scenario causes an increase of Ra. In other regions, the impacts of the different types of temperature change scenarios on Ra are similar (Fig. 2e1 and f1).

The difference responses of Ra to the different types of temperature change scenarios originate from the different response among leaf, sapwood, root and growth respiration. Ra satisfies the following equation:

$$\mathrm{Ra} = \mathrm{Rl} + \mathrm{Rs} + \mathrm{Rr} + \mathrm{Rg}$$

where Rl represents leaf respiration; Rs represents sapwood respiration; Rr represents root respiration; and Rg represents growth respiration. Rg is given by the below formula:

$$\mathrm{Rg} = \max((\mathrm{GPP}-\mathrm{R}) \times 0.25, 0),$$

where R=Rl+Rs+Rr. Maximum means that the growth respiration is always non-negative.

In southern China, Rl, Rs and Rr decrease due to the CNOP-P-type temperature change scenario which may occur because the temperature variability restrains respiration in leaves, sapwood and roots. Rg is increased due to the increasing GPP. The increasing in Rg does not offset the declines in R, so Ra decreases. However, R increases due to the linear temperature change scenario, and the extent of the increase in R is lower than for the GPP. These bring to the increases in Rg and Ra. In northeastern and northern China, the variations in Rl, Rs, Rr and Rg are similar under the two types of temperature change scenarios. The above results show that the variation in temperature variability plays an important role in autotrophic respiration in southern China.

Based on the above numerical results, a nonlinear character of the variations in annual NPP has been shown, and seasonal NPP has been simulated with the LPJ model. Thus, the seasonal variations are discussed related to the two types of temperature change scenarios. Figure 3a-k shows that the characteristics of the variations in seasonal NPP due to the two types of the temperature change scenarios are similar in spring and winter. In summer and autumn, the variations are analogous in northern and northeastern China. However, the response of NPP to the CNOP-P-type temperature change scenario is positive, while the response to the linear temperature change scenario is minor in southern China (Fig. 3a–k). The common features of the variation in NPP lie in the decreases observed in arid and semi-arid regions in the northern China in summer and autumn. In terms of GPP (Fig. 3i-p) and Ra (Fig. 3q–x), the main differences stem from the variations of Ra in southern China in summer and autumn.

3.2 Response of NPP to the CNOP-P-type precipitation change scenario

3.2.1 Impacts of the nonlinear precipitation change scenario on NPP

In this section, the response of NPP to the nonlinear precipitation change scenario is investigated. The numerical results show that total NPP increases. The increase in NPP is visible in Inner Mongolia and part of northern China, where arid and semi-arid regions are found. In contrast, in southern and northeastern China, NPP was slightly reduced. In northern China, the change in NPP was intense (Fig. 2a2 and b2). The above results reveal the variation of NPP is sensitive to the nonlinear precipitation change scenario in northern China.

3.2.2 Comparison of the impacts of the nonlinear and linear precipitation change scenarios on NPP

The impact of the linear precipitation change scenario on NPP is also discussed in comparison with that of the CNOP-P-type precipitation change scenario. It as shown that the

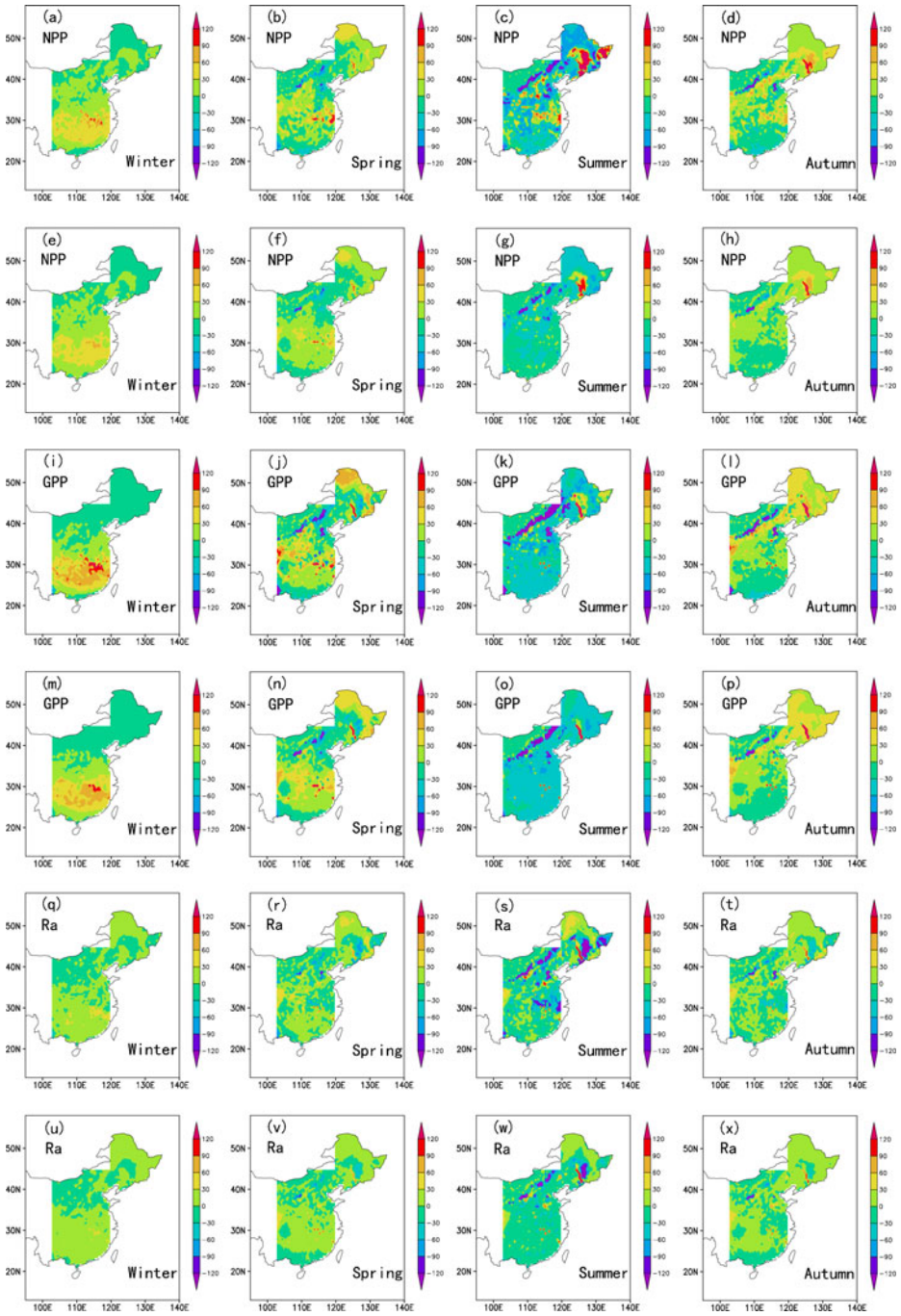

Fig. 3 The variation in NPP, GPP and Ra in comparison with the reference state in the different seasons (unit: g C m^{-2} $year^{-1}$). (**a**), (**b**), (**c**), (**d**), (**i**), (**j**), (**k**), (**l**), (**q**), (**r**), (**s**) and (**t**): the CNOP-P-type temperature changes; (**e**), (**f**), (**g**), (**h**), (**m**), (**n**), (**o**), (**p**), (**u**), (**v**), (**w**) and (**x**): the linear type temperature changes. Winter (December, January, February); spring (March, April, May); summer (June, July, August); autumn (September, October, November)

impacts of the two types of precipitation change scenarios were analogous. NPP increased in Inner Mongolia and part of northern China, while decreased in southern and northeastern China. The range of variation in response to the nonlinear precipitation change scenario was greater compared to the linear precipitation change scenario. The relative changes in NPP were also semblable. In northern China, the increase in precipitation leads to plant growth. The sensitivity of NPP in northern China is strong, which is in accord with the previous studies (Gao et al. 2000).

GPP and Ra were also examined to analyze the causes of the variation in NPP. Figure 2c2-f2 shows that the spatial variations in GPP and Ra were similar. In northern China, the increase in precipitation accelerates photosynthesis, especially in arid and semi-arid regions. In southern and northeastern China, the increase of precipitation causes a decrease in GPP and restrains the photosynthesis. In most of China, the increase of precipitation accelerates respiration.

3.3 Response of NPP to the combined temperature and precipitation change scenario

To discuss the response of NPP to combined temperature and precipitation scenarios, the LPJ model is run with combined CNOP-P-type temperature and CNOP-P-type precipitation scenarios. The two scenarios are obtained in Section 3.1 and 3.2. Figure 2a3-f3 shows that the variation in NPP is complex. In general, NPP increased in northeastern China and southern China, though it decreased slightly in parts of two regions. In northern China, the increase in NPP was clear, but reduced NPP was also visible. The response to the combined temperature and precipitation scenarios as different compared to temperature or precipitation alone. In northeastern China, the positive feedback of NPP in response to a temperature or precipitation scenario alone led to increased NPP compared to the combined temperature and precipitation scenarios. However, the positive feedback of NPP to precipitation scenarios and the negative feedback of NPP to temperature scenarios led to reduced NPP. The magnitude of reduced NPP in response to the combined temperature and precipitation scenario was lower compared to the temperature scenario alone. This implies that the positive response of NPP to precipitation could offset the loss of NPP due to the increasing temperature. This characteristic was also observed in southern China. However, in the arid and semi-arid regions of northern China, there were different results observed. In some regions, the positive impact on NPP due to the increased precipitation and the negative impact on NPP because of the increased temperature induced a positive response of NPP to the combined temperature and precipitation scenarios. These numerical results reveal that precipitation has a key modulation effect on the variation of NPP in the arid and semi-arid regions of northern China.

The annual NPP also is shown to allow discussion of the different responses to the different scenarios (Fig. 2g–i). The annual NPP due to the CNOP-P-type or linear type precipitation scenario was higher than the reference NPP, whereas the annual NPP under the linear type temperature scenario was lower than the reference NPP. However, the NPP under the CNOP-P-type temperature scenario was lower than the reference NPP before 1967. After 1967, the NPP associated with the CNOP-P-type temperature scenario was higher than the reference NPP as a result of gradually increasing temperature. The timing of the positive response to the combined CNOP-P-type temperature and precipitation scenarios was advanced due to the positive response of NPP to precipitation. The annual GPP decreased due to the temperature scenarios, whereas it increased under the precipitation scenario and the combined temperature and precipitation scenarios. The precipitation scenario and the combined temperature and precipitation scenarios also accelerated the autotrophic respiration. However, before 1964, the

temperature scenario accelerated autotrophic respiration. After 1964, the temperature scenario restrained autotrophic respiration.

4 Summary and discussion

Our objective was to consider the nonlinear response of NPP in China to climate change scenarios using the CNOP-P approach. Our main conclusions were as follows:

(1) The temperature variability fluctuates under the CNOP-P-type perturbation. The CNOP-P-type temperature change scenario causes a reduction of NPP in northern China, but increases in northeastern and southern China. The linear temperature change scenario has a similar effect. The greatest difference between the variations caused by the nonlinear and linear change scenarios occurs in southern China. The impacts of the CNOP-P-type temperature change scenario on NPP and its relative variation are larger than those of the linear temperature change scenario. The seasonal analysis reveals that NPP will decrease in summer and autumn in the arid and semi-arid regions of northern China due to climate warming. In southern China, the variation of NPP in summer and autumn is intense under the nonlinear temperature change scenario.
(2) The variability in precipitation also varies under the CNOP-P-type perturbation. The two types of precipitation change scenarios cause an increase of NPP in Inner Mongolia and part of northern China, and a reduction in northeastern and southern China.

We found that there are large differences about the variations of NPP due to two types of temperature change scenarios in southern China. Thus, the both temperature change scenarios are analyzed in southern China. In southern China, NPP increases due to the CNOP-P-type temperature change scenario. However, the variation in NPP is slight due to the linear type temperature change scenario. The average temperature in the regions is calculated. We find that the frequency of cold events due to the CNOP-P-type temperature change scenario is higher than due to the linear type temperature change scenario. For example, the temperature decreases by 0.41, 0.77 and 1.07 °C in the second year, and the late two years, respectively, due to the CNOP-P-type change scenario, while it increases by 0.06 in the second year and decreases by 0.71 and 0.31 in the last two years due to the linear type change scenario. The CNOP-P-type temperature change leads to increasing temperature variability and an increasing frequency of cold events. The increasing frequency of cold event restrains plant respiration, so the respiration of leaves, stems and roots decreases. Finally, Ra decreases, and NPP increases.

In this study, our aim was to search for a type of climate scenario that causes the maximal impact on NPP under global warming. The LPJ model is able to reproduce inter-annual variability of NPP (Sun 2009). Gao and Zhang (1997) and Gao and Yu (1998) also generated several different simple climate scenarios and explored their impacts on the vegetation dynamics in a Northeast China Transect (NECT), which was similar to, but smaller than our study region. Their research indicated that NPP decreased by 41.8 % and 34.5 % when the temperature increased by 4 °C, and NPP increased by 14.3 % and 11.5 % when the precipitation increased by 20 %. These results are similar to those of the present study obtained using a linear climate scenario. In our study, NPP was found to decrease by 1 % when the temperature increased by 2 °C and to increase by 2.3 % when precipitation increased by 20 %. The extent of variation in NPP between our study and previous studies is different because the study region and the vegetation model examined are different. However, the variation in NPP shows a large discrepancy under the CNOP-P-type

temperature scenario. NPP increases by 5.4 % due to the CNOP-P-type temperature scenario. These numerical results are similar to observational findings. Peng et al. (2010) stated that NPP shows a significant positive correlation with air temperature and precipitation in most of southeastern China based on moderate-resolution imaging spectroradiometer data (Fik and Mulligan 1998; Tian et al. 1998). In this region, our numerical results were similar to these previous findings, though some differences were observed. In our analyses, NPP was found to decrease due to increasing temperatures in the northeast part of southeastern China, which may be due to temperature variability restraining photosynthesis. In the southern part of southeastern China, NPP decreases due to increasing precipitation. The possible reasons for this result are an acceleration of autotrophic respiration due to precipitation variability, which is similar to what was proposed by Mohamed et al. (2004) who suggested that increasing precipitation variability will induce greater declines of NPP among tropical plants. In fact, the GCM output also supplies a possible climate scenario that generates variation in NPP. The effect of climate change on NPP is a combined effect of precipitation, temperature and other environmental factors. There are many studies addressing the response of terrestrial ecosystems to the combined effects of precipitation, temperature and other environmental factors (Wu et al. 2010). Medvigy et al. (2010) indicated that changes in precipitation play a key role in carbon storage and ecosystem structure, whereas temperature variability has minor influence by comparison. In contrast to these studies, our numerical results emphasize that temperature variability has a greater impact on terrestrial ecosystems than precipitation variability. A prominent trait of the CNOP-P approach is its ability to find the maximal response of terrestrial ecosystems to changes in the temperature or precipitation variability (Knapp and Smith 2001). Therefore, the changes in temperature variability observed in these previous studies and our analyses are different. The CNOP-P approach supplies a possible climate scenario that leads to the maximal impact on terrestrial ecosystems. In the previous study, the responses of NPP to temperature or precipitation changes were found to be individual. Although new variation characteristics were found, the combined effect due to environmental factors will be discussed in future works. Here, our goal is to discuss the response of NPP to climate change using a nonlinear optimization approach. We obtained the maximum value without gradients of the cost function. To calculate the optimal value, many initial values obtained through guessing were applied. The optimal value was also checked to obtain the maximal value for the cost function. Therefore, we confirm the veracity of the optimal value. Based on the above two factors, it is difficult to obtain an optimal value due to a high-dimensional optimization problem. In the present study, only the period from 1961–1970 was considered in discussing the impact of climate change on NPP. In the future, the period from 1971–2000 will be considered.

Acknowledgments The authors thank Prof. Weidong Guo for the valuable discussion and recommendation. Funding was provided by grants from LASG State Key Laboratory Special Fund and National Natural Science Foundation of China (No. 40905050, 40830955).

References

Beer C, Lucht W, Gerten D, Thonicke K, Schmullius C (2007) Effects of soil freezing and thawing on vegetation carbon density in Siberia: a modeling analysis with the Lund-Potsdam-Jena Dynamic Global Vegetation Model (LPJ-DGVM). Global Biogeochem Cycles 21:GB1012. doi:10.1029/2006GB002760

Berthelot M, Friedlingstein P, Ciais P, Dufresne JL, Monfray P (2005) How uncertainties in future climate change predictions translate into future terrestrial carbon fluxes. Glob Change Biol 11:959–970. doi:10.1111/j.1365-2486.2005.00957

Bonan GB, Levis S, Kergoat L, Oleson KW (2002) Land-scapes as patches of plant functional types: An integrated concept for climate and ecosystem models. Global Biogeochem Cycles 16(2):1021. doi:10.1029/2000GB001360

Botta A, Foley JA (2002) Effects of climate variability and disturbances on the Amazonian terrestrial ecosystems dynamics. Global Biogeochem Cycles 16(4):1070. doi:10.1029/2000GB001338

Braswell BH, Schimel DS, Linder E, Moore B III (1997) The response of global terrestrial ecosystems to interannual temperature variability. Science 278:870–872

Cao MK, Woodward FI (1998) Dynamic responses of terrestrial ecosystem carbon cycling to global climate change. Nature 393:249–252

Cao MK, Prince SD, Shugart HH (2002) Increasing terrestrial carbon uptake from the 1980s to the 1990s with changes in climate and atmospheric CO2. Global Biogeochem Cycles 16:1069. doi:10.1029/2001 GB001553

Cramer W et al (2001) Global response of terrestrial ecosystem structure and function to CO_2 and climate change: results from six dynamic global vegetation models. Glob Chang Biol 7:357–373

Collins M, Booth BB, Harris GR, Murphy JM, Sexton DMH, Webb MJ (2006) Towards quantifying uncertainty in transient climate change. Clim Dyn 27:127–147. doi:10.1007/s00382-006-0121-0

Chakraborty UK (2008) Advances in differential evolution, 1rd ed., 340 pp., Springer Verlag, Heidelberg, Berlin

Duan Q, Gupta VK, Sorooshian S (1992) Effective and effcient global optimization for conceptual rainfall-runoff models. Water Resour Res 28:1015–1031

Fay PA, Kaufman DM, Nippert JB, Carlisle JD, Harper CW (2008) Changes in grassland ecosystem function due to extreme rainfall events: implications for responses to climate change. Glob Chang Biol 14:1600–1608

Field CB, Behrenfeld MJ, Randerson JT, Falkowski P (1998) Primary production of the biosphere: integrating terrestrialand oceanic components. Science 281:237–240

Fik TJ, Mulligan GF (1998) Functional form and spatial interaction models. Environ Plan A 30(8):1497–1507. doi:10.1068/a301497

Gao Q, Zhang X (1997) A simulation study of responses of the northeast China transect to elevated CO_2 and climate change. Ecol Appl 7(2):470–483

Gao Q, Yu M (1998) A model of regional vegetation dynamics and its application to the study of Northeast China Transect (NECT) responses to global change. Global Biogeochem Cycles 12(2):329–344. doi:10.1029/97GB03659

Gao Q, Yu M, Yang X (2000) An analysis of sensitivity of terrestrial ecosystems of China to climatic change using spatial simulation. Climate Change 47:373–400

Gerber S, Joos F, Prentice IC (2004) Sensitivity of a dynamic global vegetation model to climate and atmospheric CO_2. Glob Chang Biol 7:357–373

Hu ZZ, Yang S, Wu R (2003) Long-term climate variations in China and global warming signals. J Geophys Res 108(D19):4614. doi:10.1029/2003JD003651

IPCC (2007) Summary for policymakers. In: Climate change 2007: impacts, adaptation and vulnerability. Contribution of working group II to the fourth assessment report of the intergovernmental panel on climate change. Cambridge University Press: Cambridge, New York

Ji J, Huang M, Li K (2008) Prediction of carbon exchanges between China terrestrial ecosystem and atmosphere in 21st century. Sci China Ser D 51(6):885–898

Kharin VV, Zwiers FW, Zhang X, Hegerl GC (2007) Changes in temperature and precipitation extremes in the IPCC ensemble of global coupled model simulations. J Clim 20:1419–1444

Kicklighter DW et al (1999) A first-order analysis of the potential role of CO2 fertilization to affect the global carbon budget: a comparison of four terrestrial biosphere models. Tellus 51B:343–366

Kharin VV, Zwiers FW (2000) Changes in the extremes in an ensemble of transient climate simulations with a coupled atmosphere–ocean GCM. J Clim 13:3760–3788

Knapp AK, Smith MD (2001) Variation among biomes in temporal dynamics of aboveground primary production. Science 291:481–484

Kruger J (1993) Simulated annealing-a tool for data assimilation into an almost steady model state. J Phys Oceanogr 23(4):679–688

Lotsch A, Friedl MA, Anderson BT, Tucker CJ (2003) Coupled vegetation-precipitation variability observed from satellite and climate records. Geophys Res Lett 30(14):1774. doi:10.1029/2003GL017506

Matthews HD, Weaver AJ, Meissner KJ (2005) Terrestrial carbon cycle dynamics under recent and future climate change. J Clim 18:1609–1628

Medvigy D, Wofsy SC, Munger JW, Moorcroft PR (2010) Responses of terrestrial ecosystems and carbon budgets to current and future environmental variability. Proc Natl Acad Sci USA 107(18):8275–8280

Mitchell SW, Csillag F (2001) Assessing the stability and uncertainty of predicted vegetation growth under climatic variability: northern mixed grass prairie. Ecol Model 139:101–121

Mitchell TD, Jones PD (2005) An improved method of constructing a database of monthly climate observations and associated high-resolution grids. Int J Climatol 25(6):693–712

Mohamed MAA, Babiker IS, Chen ZM, Ikeda K, Ohta K, Kato K (2004) The role of climate variability in the inter-annual variation of terrestrial net primary production (NPP). Sci Total Environ 332:123–137

Mu M, Duan WS, Wang B (2003) Conditional nonlinear optimal perturbation and its applications. Nonlinear Processes Geophys 10:493–501

Mu M, Duan WS, Wang B (2007a) Season-dependent dynamics of nonlinear optimal error growth and El Nino- Southern oscillation predictability in a theoretical model. J Geophys Res 112, D10113. doi:10.1029/2005JD006981

Mu M, Wang HL, Zhou FF (2007b) A Preliminary application of conditional nonlinear optimal perturbation to adaptive observation. Chinese J Atmos Sci (inChinese) 31(6):1102–1112

Mu M, Wang B (2007) Nonlinear instability and sensitivity of a theoretical grassland ecosystem to finite-amplitude perturbations. Nonlin Processes Geophys 14:409–423

Mu M, Duan W, Wang Q, Zhang R (2010) An extension of conditional nonlinear optimal perturbation approach and its applications. Nonlin Processes Geophys 17:211–220. doi:10.5194/npg-17-211-2010

Ni J, Sykes MT, Prentice IC, Cramer W (2000) Modeling the vegetation of China using the process-based equilibrium terrestrial biosphere model BIOME3. Glob Ecol Biogeogr 9(6):463–479

Notaro M, Vavrus S, Liu Z (2007) Global vegetation and climate change due to future increases in CO_2 as projected by a fully coupled model with dynamic vegetation. J Climate 20(1):70–90

Peng DL, Huang JF, Huete AR et al (2010) Spatial and seasonal characterization of net primary productivity and climate variables in southeastern China using MODIS data. J Zhejiang Univ-Sci B (Biomed Biotechnol) 11:275–285

Prentice IC, Cramer W, Harrison SP et al (1992) A global biome model based on plant physiology and dominance, soil properties and climate. J Biogeogr 19:117–134

Schaphoff S, Lucht W, Gerten D, Sitch S, Cramer W, Prentice IC (2006) Terrestrial biosphere carbon storage under alternative climate projections. Clim Chang 74(1–3):97–122. doi:10.1007/s10584-005-9002-5

Sitch S et al (2003) Evaluation of ecosystem dynamics, plant geography and terrestrial carbon cycling in the LPJ Dynamic Vegetation Model. Glob Chang Biol 9:161–185

Storn R, Price K (1997) Differential evolution—a simple and effcient heuristic for global optimization over continuous spaces. J Glob Optim 11:341–359

Sun G (2009) Simulation of Potential Vegetation Distribution and Estimation of Carbon Flux in China from 1981 to 1998 with LPJ Dynamic Global Vegetation Model[J]. Clim Environ Res(in Chinese) 14(4):341–351

Sun GD, Mu M (2009) Nonlinear feature of the abrupt transitions between multiple equilibria states of an ecosystem model. Adv Atmos Sci 26(2):293–304. doi:10.1007/s00376-009-0293-8

Sun G, Mu M (2011) Nonlinearly combined impacts of initial perturbation from human activities and parameter perturbation from climate change on the grassland ecosystem. Nonlin Processes Geophys 18:883–893. doi:10.5194/npg-18-883-2011

Sun GD, Mu M (2012) Responses of soil carbon variation to climate variability in China using the LPJ model. Theor Appl Climatol. doi:10.1007/s00704-012-0619-9

Tian H, Melillo JM, Kicklighter DW, McGuire AD, Helfrich JVK, Moore B, Vörösmarty CJ (1998) Effect of interannual climate variability on carbon storage in Amazonian ecosystems. Nature 396(6712):664–667

Wolf A, Blyth E, Harding R, Jacob D, Keup-Thiel E, Goettel H, Callaghan T (2008) Sensitivity of an ecosystem model to hydrology and temperature. Clim Chang 87:75–89

Wu S, Dai E, Huang M, Shao X, Li S, Tao B (2007) Ecosystem vulnerability of China under B2 climate scenario in the 21st century. Chin Sci Bull 52(10):1379–1386

Wu S, Yin Y, Zhao D, Huang M, Shao X, Dai E (2010) Impact of future climate change on terrestrial ecosystems in China. Int J Climatol 30:866–873

Zeng N, Ding Y, Pan J, Wang H, Gregg J (2008) Climate change: the Chinese challenge. Science 319:730–731

Zhang S, Zou X, Ahlquist J, Navon IM, Sela JG (2000) Use of differentiable and nondifferentiable optimization algorithms for variational data assimilation with discontinuous cost functions. Mon Weather Rev 128(12):4031–4044

Zhang X, Srinivasan R, Zhao K, Liew MV (2009) Evaluation of global optimization algorithms for parameter calibration of a computationally intensive hydrologic model. Hydrol Process 23:430–441

Zobler L (1986) A world soil file for global climate modelling, NASA Technical Memorandum, 87802, NASA, Washington, D.C., 32 pp

Zwiers FW, Kharin VV (1998) Changes in the extremes of the climate simulated by the CCC GCM2 under CO_2 doubling. J Climate 11:2200–2222